

Dalton Transactions

Accepted Manuscript



This is an *Accepted Manuscript*, which has been through the Royal Society of Chemistry peer review process and has been accepted for publication.

Accepted Manuscripts are published online shortly after acceptance, before technical editing, formatting and proof reading. Using this free service, authors can make their results available to the community, in citable form, before we publish the edited article. We will replace this *Accepted Manuscript* with the edited and formatted *Advance Article* as soon as it is available.

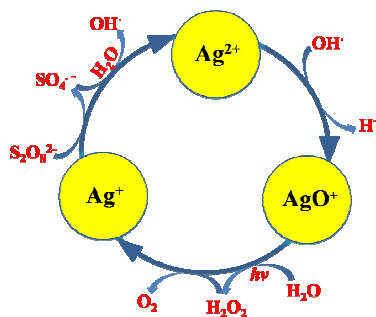
You can find more information about *Accepted Manuscripts* in the [Information for Authors](#).

Please note that technical editing may introduce minor changes to the text and/or graphics, which may alter content. The journal's standard [Terms & Conditions](#) and the [Ethical guidelines](#) still apply. In no event shall the Royal Society of Chemistry be held responsible for any errors or omissions in this *Accepted Manuscript* or any consequences arising from the use of any information it contains.

Kinetics and Mechanism of Photo-Assistant Ag(I)-Catalysed Water Oxidation with $S_2O_8^{2-}$

Lihong Yu, Jidan Wang, Dan Guo, Wansheng You,* Meiyong Liu, Lancui Zhang, and Can Li*

The kinetics of photo-assistant Ag(I)-catalysed water oxidation into O_2 with $S_2O_8^{2-}$ has been investigated. It is found that the visible light ($\lambda \geq 400$ nm) can improve the evolution of O_2 remarkably. A reasonable mechanism of Ag(I)-catalyzed water oxidation with $S_2O_8^{2-}$ has been proposed, in which the reaction ($AgO^+ + H_2O \rightarrow Ag^+ + H_2O_2$) is considered as the rate-determined step. The increase of the O_2 -evolution rate under visible light illumination results from the absorbance of the AgO^+ species at 375 nm, promoting the rate-determined reaction.



Cite this: DOI: 10.1039/c0xx00000x

www.rsc.org/xxxxxx

ARTICLE TYPE

Kinetics and Mechanism of Photo-Assistant Ag(I)-Catalysed Water Oxidation with $S_2O_8^{2-}$

Lihong Yu,^a Jidan Wang,^a Dan Guo,^a Wansheng You,^{*a} Meiyong Liu,^a Lancui Zhang,^a and Can Li^{*b}

Received (in XXX, XXX) Xth XXXXXXXXXX 20XX, Accepted Xth XXXXXXXXXX 20XX

DOI: 10.1039/b000000x

The kinetics of photo-assistant Ag(I)-catalysed water oxidation into O_2 with $S_2O_8^{2-}$ has been investigated. When the concentration of Ag^+ is less than $7.06 \times 10^{-3} \text{ mol L}^{-1}$, the O_2 -evolution rate under visible light illumination ($\lambda \geq 400 \text{ nm}$) is a first-order law with the concentrations of Ag^+ and $S_2O_8^{2-}$, respectively. The rate law is expressed as: $-dc(S_2O_8^{2-})/dt = 2dc(O_2)/dt = k_L c(S_2O_8^{2-}) c(Ag^+)$, where k_L is $12.4 \pm 1 \text{ mol}^{-1} \text{ L h}^{-1}$ at $24.5 \text{ }^\circ\text{C}$ and the activity energy is $3.7 \times 10^4 \text{ J mol}^{-1}$. It is found that the visible light can improve the evolution of O_2 remarkably. Compared with those without illumination, the rate constants under visible light are increased by *ca.* $3.8 \text{ mol}^{-1} \text{ L h}^{-1}$ at $4.5, 11.5, 17.5$ and $24.5 \text{ }^\circ\text{C}$, which are hardly effected by the reaction temperature. Employing MS/MS, ESR, XRD and UV-visible spectroscopy, the intermediate species of $\{AgS_2O_8\}^{\cdot-}$, Ag^{2+} , OH^{\cdot} , Ag_2O_3 and AgO^+ in the process of water oxidation have been detected. Based on the experimental evidences, the mechanism of Ag(I)-catalysed water oxidation with $S_2O_8^{2-}$ has been developed, in which the reaction ($AgO^+ + H_2O \rightarrow Ag^+ + H_2O_2$) is considered as the rate-determined step. The increase of the O_2 -evolution rate under visible light illumination results from the absorbance of the AgO^+ species at 375 nm , promoting the rate-determined reaction.

Introduction

Efficient water oxidation into O_2 is a bottleneck in the production of H_2 fuel from water splitting and in the reduction of CO_2 by electrolysis, photocatalysis, photoelectrocatalysis, and other approaches. Therefore, much more attention has been paid to developing viable water oxidation catalysts (WOCs)¹⁻⁴. Since the Meyer and co-workers' report of the 'blue dimer' *cis,cis*- $[(bpy)_2(H_2O)Ru^{III}ORu^{III}(H_2O)(bpy)_2]^{4+}$,⁵ a range of homogeneous metal-organic complex WOCs containing the transition metals (Ru, Ir, Co, Mn, etc.) have been reported sequentially⁶⁻¹⁶. Much great progress has been made in the activity and stability of WOCs, as well as understanding their catalytic mechanisms. Recently, Sun et al.¹⁷ have reported a mononuclear ruthenium complex $[Ru(bda)(isoq)_2]$ with catalytic activity (TOF > 300 s^{-1}) and chemical stability (TON = $8,360 \pm 91$) for water oxidation, which is moderately comparable with the reaction rate of the oxygen-evolving complex of photosystem II *in vivo*. A series of carbon-free polyoxometalate WOCs, possessing the higher stability towards oxidative degradation, have also been reported.¹⁸⁻³² In the catalytic process, central metals are oxidized into the high valent species while the aqua ligand is responsible for the proton coupled electron transfer (PCET). The high valent metal ions are responsible for the O-O forming event, and then O_2 is evolved to bring WOCs into the original state.³³⁻⁴¹

The peroxydisulfate ion ($S_2O_8^{2-}$) is not only one of frequently-used sacrificial electron acceptors to evaluate the WOCs' activity and stability,^{19,21,25,27,28,30,31,42} but also a general oxidizing agent to oxidize inorganic and organic substances.⁴³ The oxidation reactions, involving in $S_2O_8^{2-}$, however, is slow at ordinary temperature in absence of catalysts. The silver ion is the most powerful catalyst for the reactions, including water oxidation into O_2 evolution. In 1980, Kimura et al.⁴⁴ have reported the kinetics

of the Ag(I)-catalysed water oxidation with $S_2O_8^{2-}$ without illumination, proposed a mechanism for the reaction. They have considered that the rate-determining reaction of the Ag(I)-catalysed water oxidation is the same as that of inorganic and organic substances and thought that the reaction ($Ag^+ + S_2O_8^{2-} \rightarrow Ag^{2+} + SO_4^{\cdot-} + SO_4^{2-}$) is the rate-determining reaction. This is obviously different from the modern idea of the catalytic water oxidation based transitional metal complex WOCs of Ru, Ir, Co, Mn etc., in which that the rate-determining step is considered as the formation of O-O bonds or the evolution of O_2 .³³⁻⁴¹ Therefore, it is necessary to re-recognize the true essence of the Ag(I)-catalysed water oxidation.

In our research work on the Ag(I)-catalysed water oxidation, it is found that although neither $Na_2S_2O_8$ nor $AgNO_3$ absorbs visible light, visible light can accelerate the rate of water oxidation in a solution of $Na_2S_2O_8$ and $AgNO_3$. This cannot be explained by the mechanism reported by Kimura et al. It should be an intermediate species which is responsible for the absorption of visible light, and whose reaction may be the rate-determining reaction of the Ag(I)-catalysed water oxidation. In the paper, therefore, the kinetics of photo-assistant Ag(I)-catalysed water oxidation of $S_2O_8^{2-}$ is investigated and a novel mechanism of Ag(I)-catalysed water oxidation into O_2 is proposed rationally.

Experimental

Materials and Measurement

All chemicals are of analytical grade and used without further purification. Powder X-ray diffraction measurement is recorded on a D8 Advance instrument in the angular range of $2\theta = 10-70^\circ$ at 293 K with $Cu K\alpha$ radiation. The ultraviolet-visible spectra are recorded on a Lambda 35 spectrophotometer with the conditions:

scan rate, 100 nm min⁻¹; wavelength, 800 nm-200 nm. ESR signals at 77 K and ESR signals of radicals trapped by dimethyl pyridine N-oxide (DMPO) at ambient temperature are recorded on a Bruker ESR A 200 spectrometer. After bubbling O₂ for 5 minutes, the samples are introduced into a homemade quartz cup inside the microwave cavity and illuminated with a 300 W Xe lamp (CERAMAX LX-300). The settings for the ESR spectrometer are as follows: center field, 3350.00 G; sweep width, 200 G; microwave frequency, 9.41 GHz; modulation frequency, 100 kHz; power, 10.00 mW. Magnetic parameters of the radicals are obtained from direct measurements of magnetic field and microwave frequency. The TOF mass spectra were obtained on an Agilent 6224 TOF LC/MS with the negative ESI conditions: gas temperature, 346 °C; nebulizer, 40 psig; drying gas flow, 10 L min⁻¹; fragmentor voltage, 150 V; skimmer voltage, 65 V; OCT RF Vpp, 750 V.

Catalytic water oxidation

The catalytic activity is examined in a self-made closed 500 ml Quartz reaction cell containing 100 ml of an aqueous solution of Na₂S₂O₈ and AgNO₃. The light source is a 300 W Xe lamp equipped with optical filters ($\lambda \geq 370, 380, 390, 400, 420, 500, 660$ nm). A shutter window and a water filter were placed between the Xe lamp and the reaction cell to filter infrared (IR) light illumination. The reaction is carried out under Ar atmosphere and the temperature of the reaction system is controlled by ice-water bath. The amount of the produced O₂ is analyzed using gas chromatography (with a thermal conductivity detector and an Ar carrier).

Result and Discussion

Kinetics of Ag(I)-catalysed water oxidation into O₂

The Ag(I)-catalysed water oxidation has been carried out in 100 ml of the aqueous solutions with the initial concentration of 8.82×10^{-2} mol L⁻¹ Na₂S₂O₈ and different concentrations of AgNO₃ at 24.5 °C in dark. As shown in Fig. 1, the average rates of O₂ evolution in six hours are 21.0, 47.8, 85.5, 145.0 and 221.6 $\mu\text{mol h}^{-1}$ for the Ag⁺ concentrations of $5.88 \times 10^{-4}, 1.18 \times 10^{-3}, 2.35 \times 10^{-3}, 4.71 \times 10^{-3}$ and 7.06×10^{-3} mol L⁻¹, respectively. The plots of $\ln c(\text{S}_2\text{O}_8^{2-})$ vs time shows a linear relationship (Fig. S1). This shows that the reaction is a first-order law with the concentrations of Ag⁺ and S₂O₈²⁻, respectively. The rate equation is expressed as $-dc(\text{S}_2\text{O}_8^{2-})/dt = 2dc(\text{O}_2)/dt = k_0 c(\text{S}_2\text{O}_8^{2-}) c(\text{Ag}^+)$

where k_0 represents the rate constant. According to the slopes of those lines, the rate constants are obtained (Table 1). The average rate constant at 24.5 ± 0.5 °C is 8.5 ± 1 mol⁻¹ L h⁻¹. The result is comparable with that under no illumination reported by Kimura et al.⁴⁴ However, when the concentration of Ag⁺ exceeds 1.14×10^{-2} mol L⁻¹, it is found that the rate of O₂ does not rise with the concentration of Ag⁺ and simultaneously a amount of black precipitate is formed at once.

Kinetic experiments of the Ag(I)-catalysed water oxidation have also been performed with the initial concentrations of 8.82×10^{-2} mol L⁻¹ Na₂S₂O₈ and 1.18×10^{-3} mol L⁻¹ AgNO₃ at 4.5, 11.5, 17.5 and 24.5 °C. As shown in Fig. 2, the average rates of O₂ evolution in six hours are 7.6, 17.0, 31.4 and 47.8 $\mu\text{mol h}^{-1}$ respectively. The corresponding rate constants (k_0) (see Fig. S4), are listed in Table 2. According to the Arrhenius equation, $\ln k_0 =$

$\ln A - E_a/RT$, making the plots of $\ln k_0$ vs $1/T(\text{K})$ (Fig. S3), the activation energy (E_a) is obtained to be 6.5×10^4 J mol⁻¹.

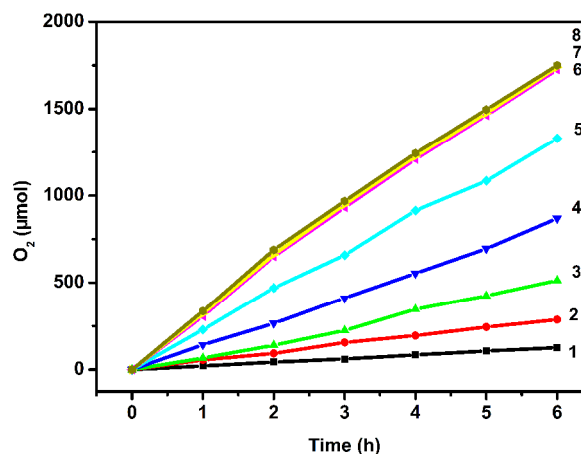


Fig. 1. Time course of O₂ evolution from 100 ml solution of AgNO₃ and Na₂S₂O₈ without illumination at 24.5 ± 0.5 °C. Na₂S₂O₈: 8.82×10^{-2} mol L⁻¹. AgNO₃: (1) 5.88×10^{-4} mol L⁻¹; (2) 1.18×10^{-3} mol L⁻¹; (3) 2.35×10^{-3} mol L⁻¹; (4) 4.71×10^{-3} mol L⁻¹; (5) 7.06×10^{-3} mol L⁻¹; (6) 9.41×10^{-3} mol L⁻¹; (7) 1.18×10^{-2} mol L⁻¹; (8) 1.41×10^{-2} mol L⁻¹.

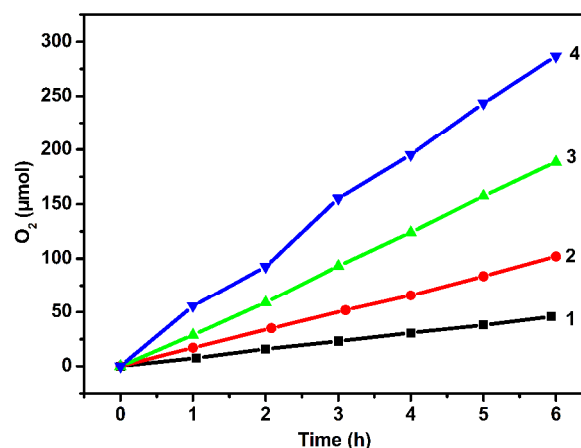


Fig. 2. Time course of O₂ evolution from 100 ml solution of AgNO₃ and Na₂S₂O₈ without illumination. Na₂S₂O₈: 8.82×10^{-2} mol L⁻¹. AgNO₃: 1.18×10^{-3} mol L⁻¹. (1) 4.5 ± 0.5 °C; (2) 11.5 ± 0.5 °C; (3) 17.5 ± 0.5 °C; (4) 24.5 ± 0.5 °C.

Kinetics of Photo-assistant Ag(I)-catalysed water oxidation into O₂

Kinetic experiments of the photo-assistant Ag(I)-catalysed water oxidation have been performed with the initial concentration of 8.82×10^{-2} mol L⁻¹ Na₂S₂O₈ and the different concentrations of AgNO₃ ($5.88 \times 10^{-4}, 1.18 \times 10^{-3}, 2.35 \times 10^{-3}, 4.71 \times 10^{-3}$ and 7.06×10^{-3} mol L⁻¹) at 24.5 °C under visible light illumination ($\lambda \geq 400$ nm). It is found that the evolution rate of O₂ is accelerated under visible light illumination. As shown in Fig. 3, the average rates of O₂ evolution in six hours are 30.2, 68.2, 120.5, 201.3 and 303.8 $\mu\text{mol h}^{-1}$ respectively. The corresponding rate constants (k_L), (see Fig. S4), are listed in Table 1. The average rate constant at 24.5 ± 0.5 °C is 12.4 ± 1 mol⁻¹ L h⁻¹.

Cite this: DOI: 10.1039/c0xx00000x

www.rsc.org/xxxxxx

ARTICLE TYPE

Table 1. The rate constants of water oxidation into O₂ for the different concentrations of Ag⁺ under no illumination and visible light (λ ≥ 400 nm) irradiation^a

Concentration of Ag ⁺ / mol L ⁻¹	Without illumination			Visible light irradiation(λ ≥ 400 nm)		
	^b S ₀	^c Rate constants k ₀ / mol ⁻¹ L h ⁻¹	Average k ₀ / mol ⁻¹ L h ⁻¹	^b S _L	^c Rate constants k _L / mol ⁻¹ L h ⁻¹	Average k _L / mol ⁻¹ L h ⁻¹
5.88×10 ⁻⁴	-0.0048	8.2(4.0%)	8.5 ± 1	-0.0070	11.9(4.3%)	12.4 ± 1
1.18×10 ⁻³	-0.0112	9.5(11.2%)		-0.0161	13.6(9.3%)	
2.35×10 ⁻³	-0.0212	9.0(5.4%)		-0.0307	13.1(5.3%)	
4.71×10 ⁻³	-0.0360	7.6(11.0%)		-0.0530	11.3(9.2%)	
7.06 ×10 ⁻³	-0.0591	8.4(1.6%)		-0.0870	12.3(1.1%)	

^aExperimental conditions: the initial concentration of Na₂S₂O₈: 8.82 × 10⁻² mol L⁻¹; at 24.5 °C; 300 W Xe equipped with an optical filter (λ ≥ 400 nm).^bS₀ and S_L represent the slopes of the lines in Fig. S1 and Fig. S3 respectively.^ck₀ and k_L = -S/c(Ag⁺).**Table 2.** The rate constants of water oxidation of S₂O₈²⁻ into O₂ at different temperatures under no light and visible light (λ ≥ 400 nm) irradiation^a

Temperature of solution (°C)	Without illumination		Visible light irradiation(λ ≥ 400 nm)		Δk = k _L - k ₀
	^b S ₀	^c Rate constant k ₀ / mol ⁻¹ L h ⁻¹	^b S _L	^c Rate constant k _L / mol ⁻¹ L h ⁻¹	
4.5 ± 0.5	-0.0018	1.5	-0.0055	4.7	3.2
11.5 ± 0.5	-0.0039	3.3	-0.0084	7.1	3.8
17.5 ± 0.5	-0.0073	6.2	-0.0118	10.0	3.8
24.5 ± 0.5	-0.0112	9.5	-0.0161	13.6	4.1

^aExperimental conditions: the initial concentration of Na₂S₂O₈: 8.82×10⁻² mol L⁻¹; the concentration of Ag⁺: 1.18×10⁻³ mol L⁻¹; 300 W Xe equipped with an optical filter (λ ≥ 400 nm).^bS₀ and S_L represent the slopes of the lines in Fig. S2 and Fig. S4 respectively.^ck₀ and k_L = -S/c(Ag⁺).

Kinetic experiments of the photo-assisted Ag(I)-catalysed water oxidation have also been performed with the initial concentrations of 8.82 × 10⁻² mol L⁻¹ Na₂S₂O₈ and 1.18 × 10⁻³ mol L⁻¹ AgNO₃ at 4.5, 11.5, 17.5 and 24.5 °C. As shown in Fig. 4, the average rates of O₂ evolution in six hours are 22.45, 36.22, 50.30, and 68.16 μmol h⁻¹ respectively. The rate constants (k_L), coming from Fig. S5, are listed in Table 2 and the corresponding activation energy (E_a) is 3.7 × 10⁴ J mol⁻¹ (see Fig. S6). The rate equation is also expressed as

$$-dc(S_2O_8^{2-})/dt = 2dc(O_2)/dt = k_L c(S_2O_8^{2-}) c(Ag^+)$$

Where k_L represents the rate constant under visible light illumination.

Compared with Ag(I)-catalysed water oxidation without illumination, it is found that visible light can improve the reaction obviously. The differences between k_L and k₀ at 4.5, 11.5, 17.5 and 24.5 °C are 3.2, 3.8, 3.8 and 4.1 respectively. Considering the experimental error, they can be regarded as a constant and the average value is 3.8 approximately. This result illustrates that the visible light-increased rates do not vary with the temperature, which is in accord with the law of photochemical reaction.

35 The mechanism of Ag(I)-catalysed water oxidation into O₂ with S₂O₈²⁻

As known, the Ag⁺ ion is the most powerful catalyst in oxidizing both inorganic and organic substances by S₂O₈²⁻. The catalytic universality and high-efficiency of Ag⁺ result from the coexistence of Ag(II) and Ag(III) species as well as radical species generated from Equations 1-5. It is believed that the rate of the oxidation reactions is dependent on the generated rate of the Ag(II)/Ag(III) species or the radical species.⁴³ In other words, the rate-determined step is Equations 1 and 2.

For Ag(I)-catalysed water oxidation, however, some experimental phenomena cannot be explained by the mechanism reported by Kimura et al.⁴⁴ Therefore, we have employed modern techniques to characterize the intermediates and analyzed scientifically the experimental phenomena in Ag(I)-catalysed water oxidation. Based on those, a new mechanism of Ag(I)-catalysed water oxidation is proposed in the paper.

The time of flight mass spectrum of a solution of Na₂S₂O₈ and AgNO₃ is investigated. As shown in Fig. 5, A peak set of five mass-to-charge ratios at 298.8090, 299.8093, 300.8086, 301.8701 and 302.8061 is observed, which agrees well with the

Cite this: DOI: 10.1039/c0xx00000x

www.rsc.org/xxxxxx

ARTICLE TYPE

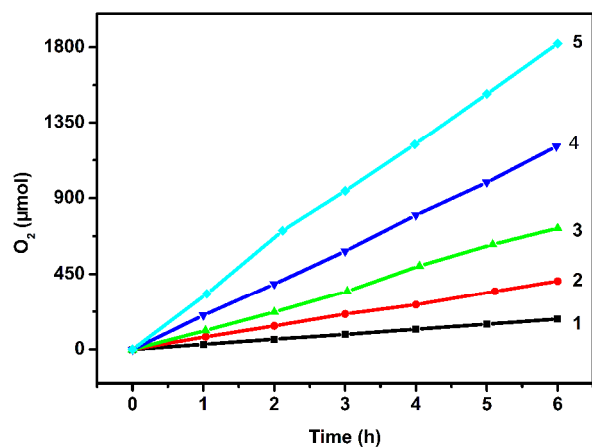


Fig. 3. Time course of O_2 evolution from 100 ml solution of $AgNO_3$ and $Na_2S_2O_8$ under the irradiation of a 300 W Xe lamp equipped with an ultraviolet cutoff filter ($\lambda \geq 400$ nm) at 24.5 ± 0.5 °C. $Na_2S_2O_8$: 8.82×10^{-2} mol L^{-1} . $AgNO_3$: (1) 5.88×10^{-4} mol L^{-1} ; (2) 1.18×10^{-3} mol L^{-1} ; (3) 2.35×10^{-3} mol L^{-1} ; (4) 4.71×10^{-3} mol L^{-1} ; (5) 7.06×10^{-3} mol L^{-1} .

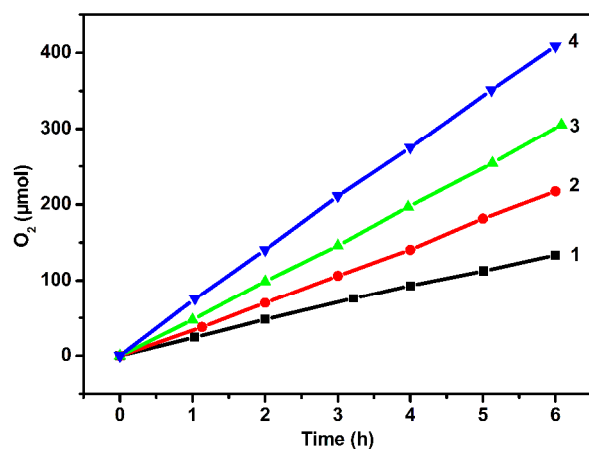


Fig. 4. Time course of O_2 evolution from 100 ml solution of $AgNO_3$ and $Na_2S_2O_8$ under the irradiation of a 300 W Xe lamp equipped with an ultraviolet cutoff filter ($\lambda \geq 400$ nm). $Na_2S_2O_8$: 8.82×10^{-2} mol L^{-1} . $AgNO_3$: 1.18×10^{-3} mol L^{-1} (1) 4.5 ± 0.5 °C; (2) 11.5 ± 0.5 °C; (3) 17.5 ± 0.5 °C; (4) 24.5 ± 0.5 °C.

fitting figure of $[Ag^+ + S_2O_8^{2-}]$. This shows that a $\{AgS_2O_8\}^-$ complex is formed in the process of Ag(I)-catalysed oxidation of water (Equation 1). This demonstrates the House's speculation, in which it is considered that the complex should be formed as an initial step of the catalytic oxidation reaction of Ag^+ ions.

ESR spectrum of the solution of $Na_2S_2O_8$ and $AgNO_3$ at 100 K is shown in Fig. 6. It consists of the three broad lines, and the anisotropic hyperfine splitting (A_{\perp}) is 29.6 G, which agrees well with those of the Ag^{2+} ions.⁴⁵⁻⁴⁷ This result confirms the existence

of Ag(II) ions in the process of Ag(I)-catalysed water oxidation. Employing DMPO as an ESR spin trap, consecutive ESR spectra of the solution $Na_2S_2O_8$ and $AgNO_3$ is obtained. As shown in Fig. 7, ESR signals are centered at $g = 2.0065$.⁴⁸⁻⁴⁹ The typical quartets with intensity of 1: 2: 2: 1 and hyperfine coupling constants of $\alpha_N = 14.9$ G and $\alpha_{H\beta} = 14.9$ G for DMPO-OH adducts appear, indicating that OH[•] radicals are formed *via* Equation 3 in the process of Ag⁺-catalysed water oxidation.

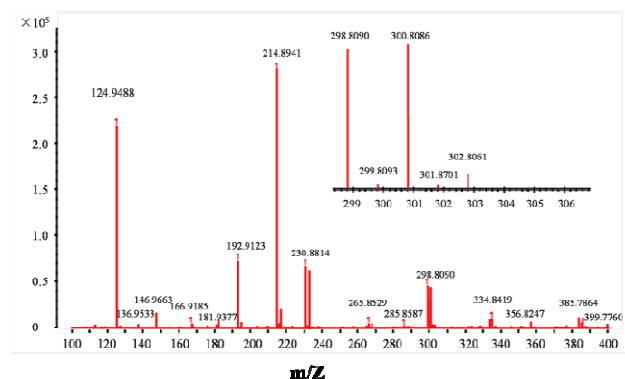


Fig. 5. Time of flight mass spectrogram for the mixed solution of 0.01 mol L^{-1} $AgNO_3$ and 0.01 mol L^{-1} $Na_2S_2O_8$. Insert: fitting figure of $[S_2O_8^{2-} + Ag^+]$.

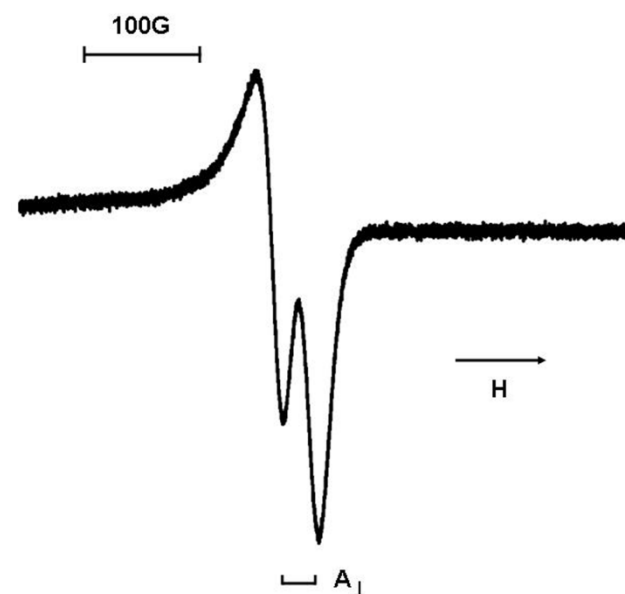


Fig. 6. ESR spectrum of a solution of $Na_2S_2O_8$ (8.82×10^{-2} mol L^{-1}) and $AgNO_3$ (1.18×10^{-3} mol L^{-1}) at 100 K.

For the aqueous solution of 8.8×10^{-2} mol L^{-1} $S_2O_8^{2-}$, when the concentration of adding Ag^+ is more than 1.41×10^{-2} mol L^{-1} , an important phenomenon is observed that the evolution rate of O_2

does not rise with the concentration of adding Ag^+ (Fig. 1), and simultaneously a black precipitate is formed as soon as the amount of Ag^+ is added. After the precipitate is washed several times with distilled water, XRD analysis indicated the presence of a single compound, which was identified as silver (III) oxide⁵⁰ (Fig.8). As early as 1926, Yost⁵¹ have employed the accurate chemical analysis to determine the precipitate to be a Ag(III) oxide, formulized as Ag_2O_3 . The Ag_2O_3 precipitate should be formed *via* a soluble Ag(III) species in the solution, recognized as AgO^+ ^{43,44,52}. As shown in Fig. 9, no absorption (> 350 nm) is observed for the individual solution of $\text{Na}_2\text{S}_2\text{O}_8$ or AgNO_3 . For the mixed solution of $\text{Na}_2\text{S}_2\text{O}_8$ and AgNO_3 , however, an obvious absorption band is observed with the maximum peak at 375 nm, which is attributed to a AgO^+ species.^{53,54} In addition, the band intensity is dependent on the concentrations of Ag^+ . This confirms the existence of Ag(III) in the process of Ag^+ -catalysed water oxidation. Because the OH^\cdot radicals has a strong oxidizing ability, it is deduced reasonably that the AgO^+ species should be generated through oxidizing Ag(II) ions with the OH^\cdot radicals. (Equation 4). Theoretically, there are two pathways to produce the AgO^+ species: (1) oxidation of Ag(II) ions with the radicals (equation 4); (2) disproportionation of Ag(II) ions (equation 6). It has been recognized generally that Equations 3, 4, 5 and 6 are fast reactions. A process of $\text{Ag}^+ \rightarrow \text{Ag}_2\text{O}_3$ can be imaged reasonably below. Firstly, Ag^+ ions are oxidized into the AgO^+ species through Equations 1-6, then the Ag_2O_3 precipitate is produced after the AgO^+ species reaches supersaturation. In this case, the evolution rate of O_2 does not increase with the concentration of adding Ag^+ . For the saturated solution of AgO^+ , its concentration should be fixed so that the evolution rate of O_2 is not changed. The experimental evidence shows that the evolution rate of O_2 is dependent on the concentration of AgO^+ . The above experimental phenomena cannot be explained by the mechanism proposed by Kimura et al.

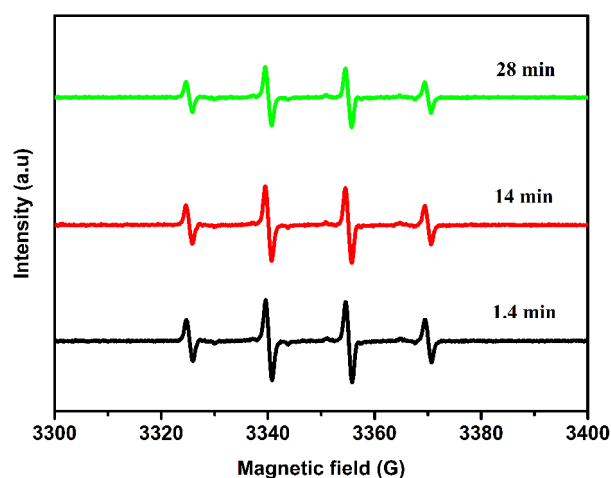


Fig. 7. In situ ESR spectra of DMPOX generated in the solution of $\text{Na}_2\text{S}_2\text{O}_8$ and AgNO_3 without illumination. The signal is denoted as '1.4 min' when the reaction is conducted for 1.4 minutes, as '14 min' for 14 minutes and as '28 min' for 28 minutes.

Compared with some Ag(I)-catalysed oxidation reactions, however, water oxidation into O_2 is much slower.⁴³ For example,

H_2O_2 is analogous to H_2O in composition, but the oxidation rate of H_2O_2 is more than one hundred times faster than that of H_2O (Fig. S6). The former differs from the later in structure that it consists of O-O bonds. If the rate-determined steps of oxidation of H_2O is the same as that of H_2O_2 , their rates of O_2 evolution should be comparable or water oxidation should be faster because water is of high concentration. The difference of the rate in their oxidation reactions may reflect from the different reaction pathways. In addition, when H_2O_2 is added to the solution of Ag^+

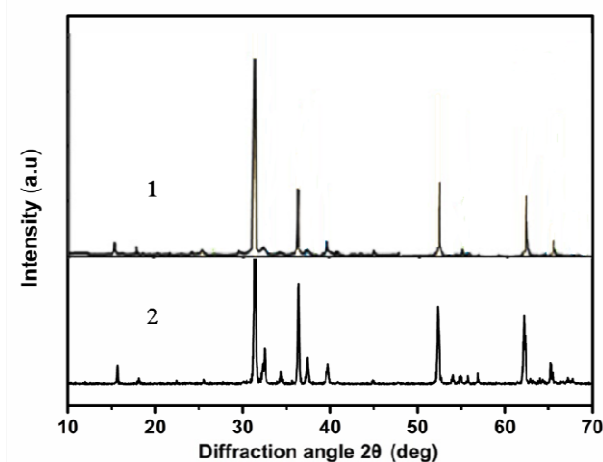


Fig. 8. XRD patterns of (1) Ag_2O_3 in Ref. 52 and (2) the black precipitate in our work, indicating the black precipitate is Ag_2O_3 .

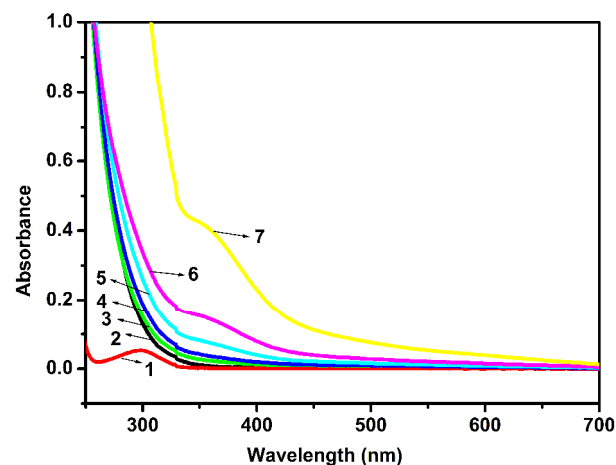
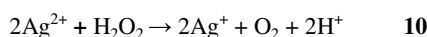
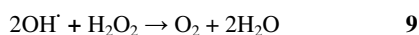
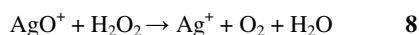
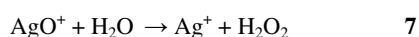
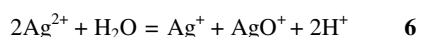
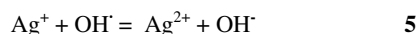
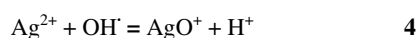
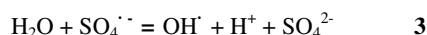
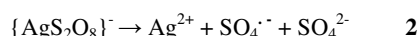


Fig. 9. UV-Visible spectra of (1) AgNO_3 ($7.06 \times 10^{-3} \text{ mol L}^{-1}$); (2) $\text{Na}_2\text{S}_2\text{O}_8$ ($8.82 \times 10^{-2} \text{ mol L}^{-1}$); (3) the solution of $\text{Na}_2\text{S}_2\text{O}_8$ ($8.82 \times 10^{-2} \text{ mol L}^{-1}$) and AgNO_3 ($1.18 \times 10^{-3} \text{ mol L}^{-1}$); (4) the solution of $\text{Na}_2\text{S}_2\text{O}_8$ ($8.82 \times 10^{-2} \text{ mol L}^{-1}$) and AgNO_3 ($2.35 \times 10^{-3} \text{ mol L}^{-1}$); (5) the solution of $\text{Na}_2\text{S}_2\text{O}_8$ ($8.82 \times 10^{-2} \text{ mol L}^{-1}$) and AgNO_3 ($4.71 \times 10^{-3} \text{ mol L}^{-1}$); (6) the solution of $\text{Na}_2\text{S}_2\text{O}_8$ ($8.82 \times 10^{-2} \text{ mol L}^{-1}$) and AgNO_3 ($7.06 \times 10^{-3} \text{ mol L}^{-1}$); (7) the filtrate of mixing $\text{Na}_2\text{S}_2\text{O}_8$ (0.1 mol L^{-1}) and AgNO_3 (0.1 mol L^{-1}).

and $\text{S}_2\text{O}_8^{2-}$, the band at 375 nm disappears immediately (Fig. S7), indicating that oxidation of H_2O_2 by AgO^+ is very fast. Therefore, this shows that the mechanism of oxidation of H_2O_2 must be different from that of H_2O . It is not entirely true that mechanism

of oxidation of water into O₂ has been considered as general oxidation of inorganic and organic substances.

In 1968, Po et al.⁵¹ proposed a concept that AgO⁺ oxidizes water into H₂O₂ while they investigated the mechanism of water oxidation by Ag(II). If the concept is introduced in the mechanism of Ag(I)-catalysed water oxidation into O₂ with S₂O₈²⁻ (equation 7), a new mechanism, involving the formation of O-O bonds, is proposed, in which equation 7 is considered as a rate-determined step. Afterwards, H₂O₂ is oxidized very fast into O₂ by Ag(II), AgO⁺ or radicals. It is not surprised that no H₂O₂ is detected in the system because the oxidation of H₂O₂ is very fast (Fig. S6).



The overall reaction:



For the mechanism, if Equation 7 is considered as a slow reaction or a rate-determined step, the experimental phenomena can be explained very well. Firstly, the Ag₂O₃ precipitate can be generated when the high concentration of Ag⁺ is employed. Secondly, the AgO⁺ species can be detected obviously in the reaction system, and Ag₂O₃ precipitate can be formed when the concentration of Ag⁺ is more than 1.41 × 10⁻² mol L⁻¹. Thirdly, the rate of Ag(I)-catalysed oxidation of water is much slower than that of H₂O₂.

Wavelength dependency of the photo-assisted Ag(I)-catalysed water oxidation have been performed in the solution of 8.82 × 10⁻² mol L⁻¹ Na₂S₂O₈ and 1.18 × 10⁻³ mol L⁻¹ AgNO₃ at 24.5 °C under the irradiation of a 300 W Xe lamp equipped with the cutoff filters of (1) λ ≥ 370 nm, (2) λ ≥ 380 nm, (3) λ ≥ 390 nm, (4) λ ≥ 400 nm, (5) λ ≥ 420 nm, (6) λ ≥ 500 nm and (7) λ ≥ 660 nm and (8) without illumination. As shown in Fig. 10 and Fig. S8, the average rates of O₂ evolution in six hours are 87.3, 76.8, 72.3, 67.8, 61.1, 49.9, 48.0 and 47.8 μmol h⁻¹ respectively. It is found that the photo-reaction system with the cutoff filter of λ ≥ 370 nm shows the highest rate obviously, and the rates are decreased gradually as the ranges of the radiation wavelength are deduced, or far away from 370 nm. When the radiation light wavelength is more than 500 nm, the rates are almost the same as that without illumination. This illustrates that the photo-assisted

catalytic water oxidation results from the AgO⁺ species. Because the absorption of the AgO⁺ species at 350 - 450 nm accelerates equation 7, so that the evolution rate of O₂ is increased by visible light illumination.

Application of the steady state hypothesis to equations 1-7 in the mechanism (see supporting information) leads to the rate law

$$dc(\text{O}_2)/dt = k c(\text{S}_2\text{O}_8^{2-}) c(\text{Ag}^+)$$

which is consistent with the experimental rate law (the concentrations of Ag⁺ are less than 1.41 × 10⁻² mol L⁻¹). Therefore, not only that, but the experimental phenomena can be explained very well. This shows that the mechanism is more reasonable. It is significant for understanding of water oxidation into O₂ and to develop high-efficiency WOCs based on silver complexes.

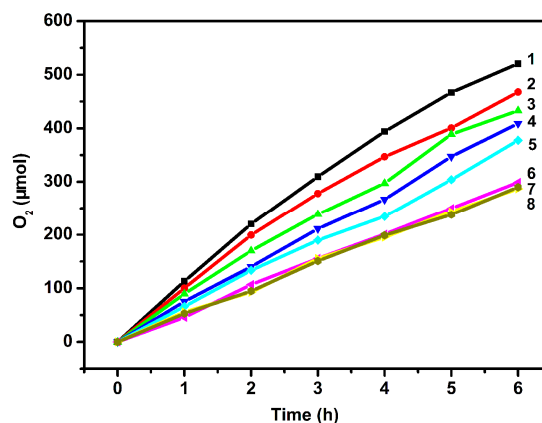


Fig. 10. Time course of O₂ evolution from 100 ml solution of AgNO₃ (1.18 × 10⁻³ mol L⁻¹) and Na₂S₂O₈ (8.82 × 10⁻² mol L⁻¹) at 24.5 ± 0.5 °C under the irradiation of a 300 W Xe lamp equipped with the cutoff filters of (1) λ ≥ 370 nm, (2) λ ≥ 380 nm, (3) λ ≥ 390 nm, (4) λ ≥ 400 nm, (5) λ ≥ 420 nm, (6) λ ≥ 500 nm and (7) λ ≥ 660 nm and (8) without illumination.

Summary

1 Visible light (λ ≥ 400 nm) can increase the rate of Ag(I)-catalysed water oxidation with S₂O₈²⁻ into O₂ further. The rate equation is -dc(S₂O₈²⁻)/dt = 2dc(O₂)/dt = k_Lc(S₂O₈²⁻)c(Ag⁺), where k_L is 8.5 ± 1 at 24.5 °C and the activation energy is ca. 3.7 × 10⁴ J mol⁻¹.

2 Based on the intermediate species of {Ag⁺...S₂O₈²⁻}, Ag²⁺, OH[·], Ag₂O₃, AgO⁺ detected in Ag(I)-catalysed water oxidation with S₂O₈²⁻, the mechanism of has been developed, where the reaction (AgO⁺ + H₂O → Ag⁺ + H₂O₂) is the rate-determined step. The increase of oxidation rate under visible light illumination results from the absorption of the AgO⁺ species at 375 nm, promoting the reaction (AgO⁺ + H₂O → Ag⁺ + H₂O₂).

3 The above results show that the high valent silver ion possesses not only the applicable potential for water oxidation, but also the ability of the formation of O-O bonds. Some silver complexes would become high-efficient WOCs.

Acknowledgment

This work is financially supported by the National Science Foundation of China (No. 20773057) and the State Key Laboratory of Fine Chemicals of China (KF 1204) and Key Laboratory of Polyoxometalates Science of Ministry of Education of China for support of this research.

Notes and references

^a Institute of Chemistry for Functionalized Materials, Liaoning Normal University, Dalian, 116029, P. R. China. Fax: +86 411 82156858; Tel: +86 411 82159378; E-mail: wsyoun@lnu.edu.cn

^b State Key Laboratory of Catalysis, Dalian Institute of Chemical Physics, The Chinese Academy of Sciences, Dalian 116023, P. R. China. E-mail: canli@dicp.ac.cn

[†] Electronic Supplementary Information (ESI) available: Plots of $\ln k(S_2O_8^{2-})$ vs. time; Plots of $\ln k$ vs. $1000/T(K)$; UV-Visible spectra of the solution of (1) $Na_2S_2O_8$ ($8.82 \times 10^{-2} \text{ mol L}^{-1}$) and $AgNO_3$ ($7.06 \times 10^{-3} \text{ mol L}^{-1}$), (2) H_2O_2 is added to (1); Steady State Analysis of the Proposed Mechanism. For ESI electronic format see DOI: 10.1039/b000000x/

- 1 J. H. Alstrum-Acevedo, M. K. Brennaman, T. J. Meyer, *Inorg. Chem.*, 2005, **44**, 6802.
- 2 L. Sun, L. Hammarström, B. Åkermark, S. Styring, *Chem. Soc. Rev.*, 2001, **30**, 36.
- 3 D. Gust, T. A. Moore, A. L. Moore, *Acc. Chem. Res.*, 2009, **42**, 1890.
- 4 R. Eisenberg, H. B. Gray, *Inorg. Chem.*, 2008, **47**, 1697.
- 5 S. W. Gersten, G. J. Samuels, T. J. Meyer, *J. Am. Chem. Soc.*, 1982, **104**, 4029.
- 6 J. J. Concepcion, M. K. Tsai, J. T. Muckerman, T. J. Meyer, *J. Am. Chem. Soc.*, 2010, **132**, 1545.
- 7 J. Nyhlén, L. L. Duan, B. Åkermark, L. C. Sun, T. Privalov, *Angew. Chem. Int. Ed.*, 2010, **49**, 1773.
- 8 X. Sala, I. Romero, M. Rodríguez, L. Escriche, A. Llobet, *Angew. Chem. Int. Ed.*, 2009, **48**, 2842.
- 9 R. Zong, R. P. Thummel, *J. Am. Chem. Soc.*, 2005, **127**, 12802.
- 10 S. W. Kohl, L. Weiner, L. Schwartzburd, L. Konstantinovskii, L. J. W. Shimon, Y. Ben-David, M. A. Iron, D. Milstein, *Science*, 2009, **324**, 74.
- 11 N. D. McDaniel, F. J. Coughlin, L. L. Tinker, S. Bernhard, *J. Am. Chem. Soc.*, 2008, **130**, 210.
- 12 H. Kunkely, A. Vogler, *Angew. Chem. Int. Ed.*, 2009, **48**, 1685.
- 13 J. Limburg, J. S. Vrettos, J. M. Liabre-Sands, A. L. Rheingold, R. H. Crabtree, G. W. Brudvig, *Science*, 1999, **283**, 1524.
- 14 W. C. Ellis, N. D. McDaniel, S. Bernhard, T. J. Collins, *J. Am. Chem. Soc.*, 2010, **132**, 10990.
- 15 Y. H. Xu, L. L. Duan, L. P. Tong, B. Åkermark, L. C. Sun, *Chem. Commun.*, 2010, **46**, 6506.
- 16 M. Yagi, K. Narita, *J. Am. Chem. Soc.*, 2004, **126**, 8084.
- 17 L. L. Duan, F. Bozoglian, S. Mandal, B. Stewart, T. Privalov, A. Llobet, L. C. Sun, *Nat. Chem.*, 2012, **4**, 418.
- 18 H. J. Lv, J. Song, Y. V. Geletii, J. W. Vickers, J. M. Sumliner, D. G. Musaev, P. Kögerler, P. F. Zhuk, J. Bacsá, G. B. Zhu, and C. L. Hill, *J. Am. Chem. Soc.*, 2014, **136**, 9268.
- 19 Y. V. Geletii, B. Botar, P. Kögerler, D. A. Hillesheim, D. G. Musaev, C. L. Hill, *Angew. Chem. Int. Ed.*, 2008, **47**, 3896.
- 20 A. Sartorel, M. Carraro, G. Scorrano, R. D. Zorzi, S. Geremia, N. D. McDaniel, S. Bernhard, M. Bonchio, *J. Am. Chem. Soc.*, 2008, **130**, 5006.
- 21 Y. V. Geletii, Z. Q. Huang, Y. Hou, D. G. Musaev, T. Q. Lian, C. L. Hill, *J. Am. Chem. Soc.*, 2009, **131**, 7522.
- 22 A. Sartorel, P. Miró, E. Salvadori, S. Romain, M. Carraro, G. Scorrano, M. D. Valentin, A. Llobet, C. Bo, M. Bonchio, *J. Am. Chem. Soc.*, 2009, **131**, 16051.
- 23 F. M. Toma, A. Sartorel, M. Iurlo, M. Carraro, P. Parisse, C. Maccato, S. Rapino, B. R. Gonzalez, H. Amenitsch, T. D. Ros, L. Casalis, A. Goldoni, M. Marcaccio, G. Scorrano, G. Scoles, F. Paolucci, M. Pratol, M. Bonchio, *Nat. Chem.*, 2010, **2**, 826.
- 24 M. Murakami, D. Hong, T. Suenobu, S. Yamaguchi, T. Ogura, S. Fukuzumi, *J. Am. Chem. Soc.*, 2011, **133**, 11605.
- 25 P. Car, M. Guttentag, K. K. Baldrige, R. Alberto, G. R. Patzk, *Green Chem.*, 2012, **14**, 1680.
- 26 Q. Yin, J. M. Tan, C. Besson, Y. V. Geletii, D. G. Musaev, A. E. Kuznetsov, Z. Luo, K. I. Hardcastle, C. L. Hill, *Science*, 2010, **328**, 342.
- 27 Z. Q. Huang, Z. Luo, Y. V. Geletii, J. W. Vickers, Q. S. Yin, D. Wu, Y. Hou, Y. Ding, J. Song, D. G. Musaev, C. L. Hill, T. Q. Lian, *J. Am. Chem. Soc.*, 2011, **133**, 2068.
- 28 M. Natali, S. Berardi, A. Sartorel, M. Bonchio, S. Campagnac, F. Scandola, *Chem. Commun.*, 2012, **48**, 8808.
- 29 S. Tanaka, M. Annaka, K. Sakai, *Chem. Commun.*, 2012, **48**, 1653.
- 30 F. Y. Song, Y. Ding, B. C. Ma, C. M. Wang, Q. Wang, X. Q. Du, S. Fu, J. Song, *Energy Environ. Sci.*, 2013, **6**, 1170.
- 31 J. Soriano-López, S. Goberna-Ferrón, L. Vigara, J. J. Carbó, J. M. Poblet, *Inorg. Chem.*, 2013, **52**, 4753.
- 32 H. Lv, Y. V. Geletii, C. Zhao, J. W. Vickers, G. Zhu, Z. Luo, J. Song, T. Lian, D. G. Musaev, C. L. Hill, *Chem. Soc. Rev.*, 2012, **41**, 7572.
- 33 J. K. Hurst, J. L. Cape, A. E. Clark, S. Das, C. Y. Qin, *Inorg. Chem.*, 2008, **47**, 1753-1764.
- 34 Z. L. Lang, G. C. Yang, N. N. Ma, S. Z. Wen, L. K. Yan, W. Guan, Z. M. Su, *Dalton Trans.*, 2013, **42**, 10617.
- 35 F. Liu, J. J. Concepcion, J. W. Jurss, T. Cardolaccia, J. L. Templeton, T. J. Meyer, *Inorg. Chem.*, 2008, **47**, 1727.
- 36 T. A. Betley, Q. Wu, T. V. Voorhis, D. G. Nocera, *Inorg. Chem.*, 2008, **47**, 1849.
- 37 D. J. Wasylenko, C. Ganesamoorthy, M. A. Henderson, C. P. Berlinguette, *Inorg. Chem.*, 2011, **50**, 3662.
- 38 D. J. Wasylenko, C. Ganesamoorthy, M. A. Henderson, B. D. Koivisto, H. D. Osthoff, C. P. Berlinguette, *J. Am. Chem. Soc.*, 2010, **132**, 16094.
- 39 G. Mattioli, P. Giannozzi, A. A. Bonapasta, L. Guidoni, *J. Am. Chem. Soc.*, 2013, **135**, 15353.
- 40 S. Romain, F. Bozoglian, X. Sala, A. Llobet, *J. Am. Chem. Soc.*, 2009, **131**, 2768.
- 41 B. S. Brunshwig, M. H. Chou, C. Creutz, P. Ghosh, N. Sutin, *J. Am. Chem. Soc.*, 1983, **105**, 4832.
- 42 Y. H. Xu, L. L. Duan, L. P. Tong, B. Åkermark, L. C. Sun, *Chem. Commun.*, 2010, **46**, 6506.
- 43 D. A. House, *Chem. Rev.*, 1962, **62**, 185.
- 44 M. Kimura, T. Kawajiri, *J. Chem. Soc. Dalton.*, 1980, 726.
- 45 T. Buch, *J. Chem. Phys.*, 1965, **43**, 761.
- 46 J. A. McMillan, B. Smaller, *J. Chem. Phys.*, 1961, **35**, 1698.
- 47 N. Kanraki, I. Yasumori, *J. Phys. Chem.*, 1978, **82**, 2351.
- 48 S. Leonard, P. M. Gannett, Y. Rojanasakul, D. Schwegler-Berry, V. Castranova, V. Vallyathan, X. L. Shi, *J. Inorg. Biochem.*, 1998, **70**, 239.
- 49 S. Stan, J. S. Woods, M. A. Daeschel, *J. Agric. Food. Chem.*, 2005, **53**, 4901.
- 50 S. Ando, T. Hioki, T. Yamada, N. Watanabe, A. Higashitani, *J. Mater. Sci.*, 2012, **47**, 2928.
- 51 D. M. Yost, *Chem. Rev.*, 1926, **48**, 152.
- 52 H. N. Po, J. H. Swinehart, T. L. Allen, *Inorg. Chem.*, 1968, **7**, 244.
- 53 J. D. Miller, *J. Chem. Soc. (A)*, 1968, 1778.
- 54 G. L. Cohen, G. Atkinson, *Inorg. Chem.*, 1964, **42**, 52.